

Spectral Analysis of Bright Gamma Ray Bursts

G. Ghirlanda^{*}, A. Celotti^{*} and G. Ghisellini[†]

^{*}*SISSA/ISAS, Trieste - Via Beirut 2, 34014 Trieste, Italy*

[†]*Osservatorio Astronomico di Brera, via Bianchi 46, Merate (LC), Italy*

Abstract. We present the time integrated and time resolved spectral analysis of a sample of bright bursts selected from the BATSE archive. We fitted four different spectral models to the time integrated and time resolved spectra of the flux pulses. We point out that the found (marginal) differences in the parameter distributions can be ascribed to the different spectral shape of the employed models and that a smoothly curved model best fits the observed spectra. We characterize the spectral shape of bright bursts and compare the low energy slope of the fitted spectra with the prediction $N(E) \propto E^{-2/3}$ of the synchrotron theory, finding that this limit is violated in a considerable number of time resolved spectra around the peaks, both during the rise and decay phase.

INTRODUCTION

The nature and emission mechanisms responsible for the prompt emission of Gamma-ray bursts (GRB) are still unclear. In order to identify the physical process(es) responsible for the emission it would be ideally necessary to study spectra resolved on the shortest time-scales of variability, typically of a few milliseconds, observed in bright bursts [3] and predicted on theoretical basis [11]. In fact time resolved spectra, even within single pulses, show a strong time evolution, and are, in general, harder than time integrated spectra [6], [2].

Here we present the study of the spectral properties of single pulses within bright GRBs, compare the results of the spectral analysis of the time average spectrum with the time resolved spectra of the very same burst in order to quantify systematic differences and examine any spectral ‘violation’ (with respect to the predicted slope in the case of e.g. synchrotron emission) for the entire burst evolution. A more detailed analysis is given in [7].

DATA ANALYSIS

The main characteristics of the BATSE detectors have been described by [3]. We selected bursts with a peak flux, on the 64 ms time-scale, higher than 20 phot/cm²sec. The data used were mainly the HERB: time sequence of 128 channel spectra with a minimum integration time of 0.128 s.

Within the selected bursts each peak was analyzed separately considering the spectrum time-integrated over the duration of the peak and the sequence of time resolved

spectra comprised within the same peak. We fitted the background subtracted spectra with 4 spectral models: the BAND one (Band et al. [1]) which consists of 2 power laws joined smoothly by an exponential roll-over, the Broken Power Law (BPLW hereafter) which has a sharp break between the two power law segments, the COMP model which comprises a low energy power law ending-up in an exponential cutoff, and the Synchrotron Shock Model (SSM) [12] based on optically thin synchrotron emission from relativistic particles (and for the first time fitted to the time resolved spectra).

RESULTS

From a statistical point of view, the comparison of the spectral fits obtained with the 4 models shows that in terms of the reduced χ^2 , the BAND and COMP models can better represent the time resolved spectra of bright bursts, but some counter examples exist showing that in general within a single pulse more than one time resolved spectrum can be fitted by different spectral models.

The parameters distributions

The distributions of the *low energy power law spectral index* α (Fig.1), for the BAND and COMP model, are similar, like in the case of the time integrated spectra, and both have a mode of -0.85 ± 0.1 , also consistent with the BPLW average value -1.15 ± 0.1 . Note that qualitatively the extension of the α distribution of the BPLW model (*solid line* in Fig.1) towards lower values

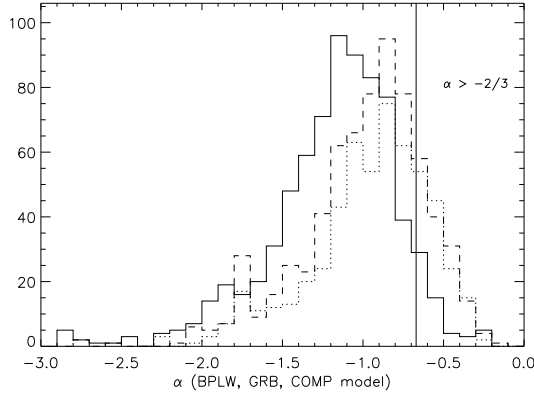


FIGURE 1. Low energy power law spectral index (α) distributions derived from the time resolved spectral analysis. *Solid line:* BPLW model, *dotted line:* BAND model, *dashed line:* COMP model. The vertical line represents the synchrotron limit ($\alpha = -2/3$) for the low energy spectral shape.

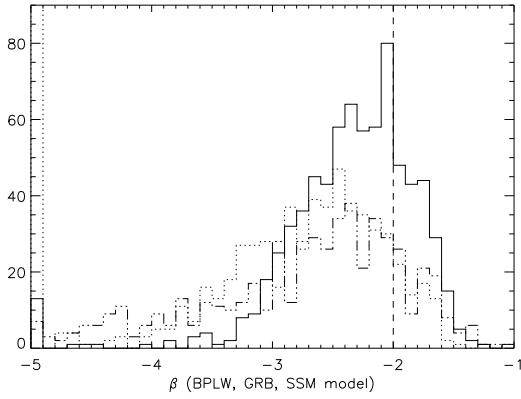


FIGURE 2. High energy power law spectral index (β) distributions for the time resolved spectra. *Solid line:* BPLW model; *dotted line:* BAND model; *dot-dashed line:* SSM model. Also shown (bin with $\beta = -5$) the time resolved spectra with undetermined high energy spectral index for the BAND model.

could be attributed to the fact that at low energies this model (which has a sharp break) tends to under-estimate the hardness of the spectrum compared to a smoothly curved model.

The average low energy spectral slope obtained from the time resolved spectra is harder than what obtained with the time integrated pulse spectra for all the three models (BAND, BPLW, COMP). This is a consequence of time integration (i.e. hardness averaging) of the spectral evolution (which can be also very dramatic) over the entire rise and decay phase of the pulse.

The *high energy spectral index* β distributions are reported in Fig.2. The average value is -2.45 ± 0.1 and

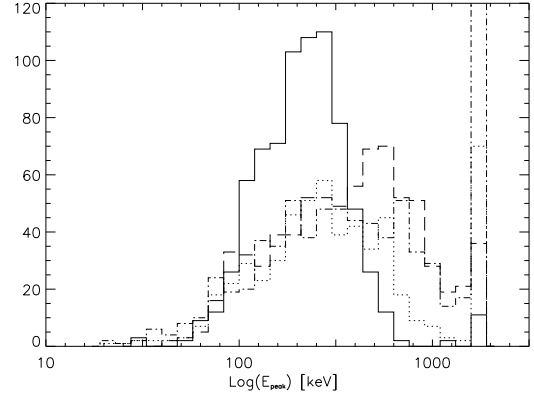


FIGURE 3. E_{peak} - Peak energy distribution for the 4 spectral models. *solid line:*BPLW model,*dotted line:*BAND model, *dashed line:*COMP model,*dot-dashed line:*SSM model. Spectra with undetermined peak energy (i.e. the high energy threshold 1800 keV assumed as lower limit) are reported in the last bin.

-2.05 ± 0.1 for the BAND and BPLW model respectively, the former being harder than what obtained from the pulse average spectrum. The SSM average β is -2.17 which is consistent with what found from the average pulse spectral analysis.

The most important spectral parameter obtained in fitting the spectrum with these models is E_{peak} corresponding to the peak of the EF_E spectrum, and thus to the energy where most of the power is released. E_{peak} is coincident with the break energy E_0 for the BPLW and COMP and is equal to $(\alpha + 2)E_0$ for the BAND model. This characteristic energy can be obviously calculated only for those spectra (BPLW and BAND model) with $\beta < -2$ and its distribution is presented in Fig.3. The average is $E_{peak} = 280^{+72}_{-57}$ keV for the BAND model, consistent, within the errors, with the BPLW most probable value of 211^{+25}_{-22} keV. The COMP model, instead, gives a highly asymmetric peak energy distribution with a mode of 595^{+104}_{-88} keV because the lack of an high energy power law component tends to over-estimate the energy corresponding to the start of the exponential cutoff. The SSM model has an average $E_{peak} \sim 316^{+64}_{-52}$ keV with a wide distribution.

The Synchrotron limit violation

A strong prediction of the optically thin synchrotron model is that the asymptotic low energy photon slope α should be lower than or equal to $-2/3$ [8].

We obtain that the 13.7% of the time resolved spectra fitted with the BAND model are inconsistent with $\alpha \leq -2/3$ at 2σ . A similar percentage of spectra violating the

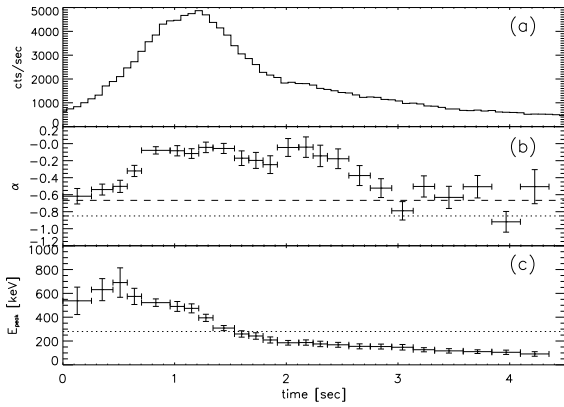


FIGURE 4. Trigger 2083. Spectral evolution of the BAND model fitted to the time resolved spectra. Light curve on the 64 ms time-scale (panel a); low energy spectral index and (*dashed*) synchrotron shock model limit $\alpha = -2/3$ (b); peak energy (c). For reference the average values of α and E_{peak} obtained from the time resolved spectra (*dotted line*) and the synchrotron model limit are reported (*dashed line*).

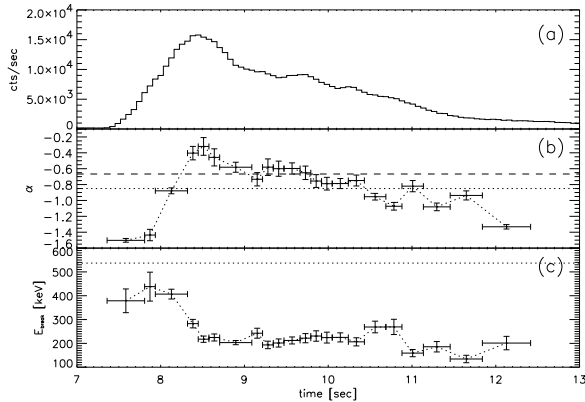


FIGURE 5. Trigger 5614. Spectral evolution of the COMP model fitted to the time resolved spectra. Light curve on the 64 ms time-scale (panel a); low energy spectral index and (*dashed*) synchrotron shock model limit $\alpha = -2/3$ (b); peak energy (c). For reference the average values of α and E_{peak} obtained from the time resolved spectra (*dotted line*) and the synchrotron model limit (*dashed line*) are reported.

α limit is found for the COMP model ($\sim 11.7\%$, of course mostly for the same spectra). Moreover $\sim 21\%$ of the time resolved peak spectra violate the synchrotron limit, indicating that this violation happens during the peak phase and not preferentially before or after it: in Fig.4 we show the spectral evolution in the case of GRB921207 (fitted with the BAND model) and another example is reported in Fig.5.

CONCLUSIONS

We considered a sample of bright burst detected by BATSE and performed a uniform analysis for the time integrated and the time resolved (typically 128 ms) spectra with four different models adopted and proposed in the literature.

We find that even at this time resolution no model can better represent the data and different spectra require different shapes, re-confirming the erratic behavior of bursts and also possibly indicating that time resolution on time-scales comparable with the variability one are needed. The parameter distributions are consistent with the results reported by [10] although the average spectral shape (both from the time resolved and time integrated spectra) is harder because we selected only bright bursts and restricted the spectral analysis to the pulse phase.

A considerable number of spectra are characterized by extremely hard low energy components with spectral index greater than $-2/3$ (i.e. the limit predicted by synchrotron theory [8]). The α limit violation, also found by [5] and [2], is evident around the peak both during the rise and decay phase, and this could indicate that at some stages of the burst evolution (possibly near the peak of emission itself) alternative radiative processes, other than synchrotron, can be dominant.

ACKNOWLEDGMENTS

This research has made use of data obtained through the High Energy Astrophysics Science Archive Research Center Online Service, provided by the NASA/Goddard Space Flight Center. We are grateful to D. Band for useful discussions on the BATSE data analysis. We thank Marco Tavani for having provided his code of the SSM model. Giancarlo Ghirlanda and AC acknowledge the Italian MUIR for financial support.

REFERENCES

1. Band D. et al., *ApJ* **413**, 281-292 (1993)
2. Crider A. et al., *ApJ* **479**, L39-L42 (1997)
3. Fishman G. J. & Meegan C. A., *ARAA* **33**,415-458 (1995)
4. Ford L. et al., *ApJ* **439**, 307-321 (1995)
5. Frontera F. et al., *ApJ* **127**, 59-78 (2000)
6. Liang E. P. & Kargatis V. E., *Nature* **318**, 495 (1996)
7. Ghirlanda G., Celotti A. & Ghisellini G., 2001, A&A submitted
8. Katz J.I., *ApJ* **432**, L107 (1994)
9. Preece R. D. et al., *ApJ* **496**, 849-862 (1998)
10. Preece R. D. et al., *ApJ SS* **126**, 19-36 (2000)
11. Rees M. J. and Meszaros P., *ApJ* **430**, L93 (1994)
12. Tavani M., *ApJ* **466**, 768-778 (1996)